Bifurcations in a sidebranch surface of a free-growing dendrite

P. K. Galenko, M. D. Krivilyov, and S. V. Buzilov
Institute of Mathematical Simulation, Udmurt State University, 71 Krasnogeroyskaya Street, Izhevsk 426034, Russian Federation
(Received 24 April 1996; revised manuscript received 14 August 1996)

We consider a model of a free-growing dendrite in a binary dilute system solidifying under nonequilibrium conditions. The numerical solution of the model equations was obtained by finite-difference technique on a two-dimensional square lattice. A special case in which the liquid-solid surface tension is zero and a stabilizing action on the dendritic form is produced by both the surface kinetics and the anisotropic influence of the computational lattice was studied. We find that, depending on the initial undercooling and computational lattice scale, an interesting behavior in the dendrite sidebranch surface is expected. Except for the evolution of the sidebranch surface realized by regularly repeated doubling of the distances between the secondary branches by the Feigenbaum scenario, there is a clear tendency for the formation of a needlelike dendrite, structured after a Hopf-type bifurcation, chaotic structure with random period of branching, packet structure with the branching period that is not defined by the Feigenbaum scenario. Simulation data are correlated with known conclusions of the thermodynamical approach to phase transformations, marginal stability theory, and analytical treatments of the local model of the boundary layer. Satisfactory qualitative agreement with the results given by the continuum diffusion-limited aggregation model and the modeling of three-dimensional heat flow dendrites has been found. [S1063-651X(97)00301-2]

PACS number(s): 05.70.Fh, 68.70.+w

I. INTRODUCTION

Dendrites are recognized as one manifestation of the structural behavior of a dissipative system in condensed media under nonequilibrium conditions [1]. The detailed study of natural dendritic growth [2] and modeling of dendritic structures [3–5] lead to an understanding of the main peculiarities of tip growth and sidebranch formation during solidification of undercooled liquids. In particular, the marginal stability theory of dendrite growth [6,7] shows that the tip is the only point on a dendrite that is stable and sidebranch formation is due to the instability of all other positions of a phase interface. Therefore, among the major types of patterns that typically occur during unstable interfacial growth, dendrites are patterns with a symmetry of varying degree and without tip splitting (see Ref. [1] and Ref. [8], pp. 277–278).

The search of the dynamical stability criteria of the dendrite tip and the condition of dendrite sidebranch surface formation lead to the general problem of mode selection in dendritic patterns [2,9]. As in pattern formation during directional solidification [10], there is a selection in the sidebranch surface of a free-growing dendrite, and the wavelength between its secondary branches depends on undercooling in a system [1–5].

In a computer model of a free-growing dendrite, Umantsev, Vinogradov, and Borisov [3] showed that the evolution of the wave sidebranch structure has a regular doubling of the period λ between the fast-growing secondary branches of the Feigenbaum scenario. The period λ varies as double increases, $\lambda \rightarrow 2\lambda \rightarrow 4\lambda$, along the main stem of the dendrite [3]. After a thermodynamical study of isolated adiabatic systems, Umantsev and Olson [11] remarkably stated that the mechanism of sequential period doubling is robust for coarsening processes in systems with a conserved quantity. In addition, Umantsev *et al.* [3] noted that, besides the Feigenbaum bifurcation, which leads to the period doubling $\lambda \rightarrow 2\lambda$ in the secondary branches of the free dendrite, the sidebranch surface can have a shorter branching period, i.e., the structure of the secondary branches becomes more dense. The dendrite can also have an abnormally long steady-state undisturbed area behind the tip [3].

In one dendritic model of Galenko and Zhuravlev [1], an increase in the period $\lambda \rightarrow 2\lambda$ for the fast-growing branches has also been found. After a smooth nonbranching area behind the tip, the surface of the needlelike crystal becomes morphologically unstable. This instability defines the origin and development of the secondary branches by a Hopf-type bifurcation scenario $\lambda \rightarrow \lambda \rightarrow \lambda$. Then the Feigenbaum transfer $\lambda \rightarrow 2\lambda \rightarrow 4\lambda$ may proceed with an intermediate stage of an accidental change of the branching period $\lambda \rightarrow 3\lambda \rightarrow 2\lambda \rightarrow 6.5\lambda \rightarrow 3\lambda$. As the initial undercooling increases, the enlargement of the lateral structure becomes the most advantageous as $\lambda \rightarrow 3\lambda \rightarrow 6\lambda$ (see Ref. [1], p. 130), and different structures of the dendrite sidebranch surface can occur.

The major purpose of this paper is to establish a possible morphological spectrum of the sidebranch surface after bifurcations in the structure of a free-growing dendrite. We show the results of computational experiments from which a variety of virtual types of dendritic sidebranch surfaces arise according to the initial undercooling in the system.

The paper is organized as follows. In Sec. II we introduce the mathematical model of dendrite growth in a binary dilute system. In Sec. III we give the results of the two-dimensional modeling the free dendrite growth. Section IV is devoted to morphologies of the dendrite sidebranch surface that evolve from deeply undercooled binary liquid. In Sec. V we discuss the results of modeling the morphological spectrum and how to grow an area nearest the tip of the free dendrite during branching of its surface. Finally, in Sec. VI we present a summary of our conclusions.

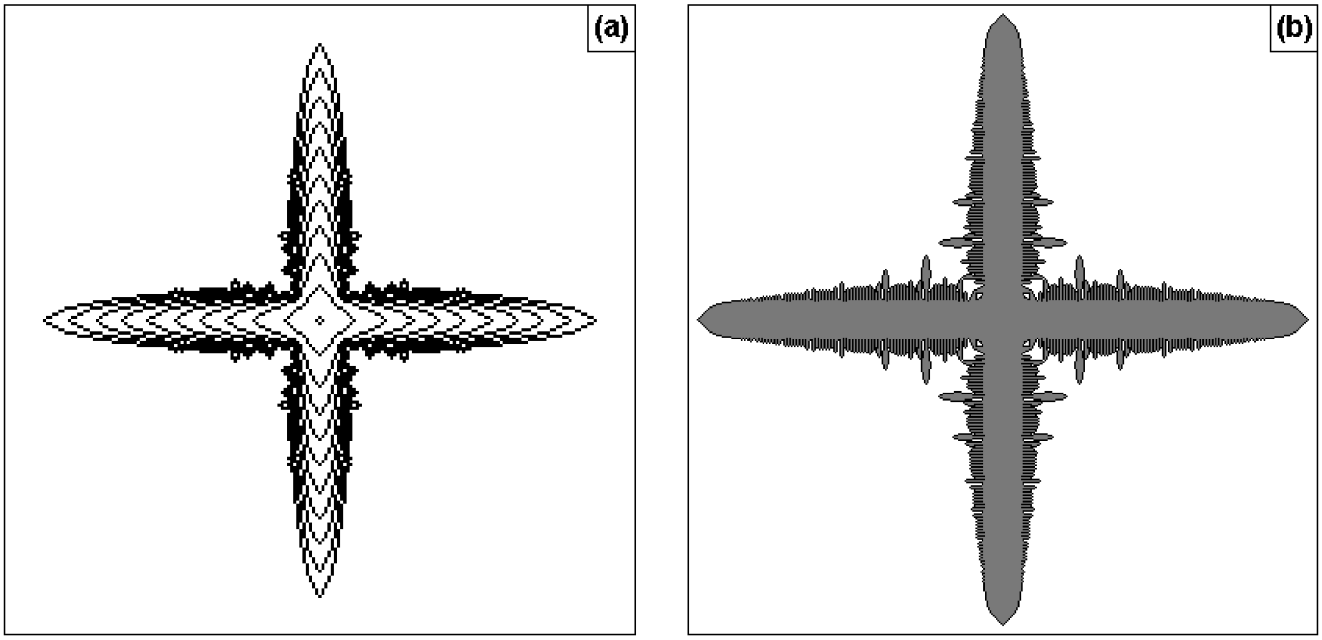

FIG. 1. Free dendrite calculated by the lattice model. The growth starts from the initial single seed of the solid phase placed at the central site of the lattice. (a) Various stages in the growth of a dendrite calculated using the initial undercooling $\delta T_0=0.64$ on the 127×127 lattice. (b) Dendritic pattern on the 221×221 lattice. The initial undercooling $\delta T_0=1.39$.

II. MODEL OF DENDRITIC GROWTH

The process of dendrite growth from a supercooled binary diluted system can be described by the continuum model [1]

$$\frac{\partial}{\partial t}[(1-G)C_L+GkC_L]=\mathrm{div}[(1-G)D_L\ \mathrm{grad}\ C_L], \quad (1)$$

$$G=1-\exp\left(-\int_t(\omega/\upsilon)V\,dt\right), \quad (2)$$

$$V=\beta(T_A-T_0-mC_L), \quad (3)$$

$$C_S=kC_L. \quad (4)$$

Here C_L and C_S are the concentrations in the liquid and solid phases, respectively, G is the solid phase fraction, D is the diffusion constant, V is the velocity of the liquid-solid interface along the normal vector pointed towards the liquid, t is the time, ω is the liquid-solid interface inside the solidifying system, υ is the two-phase bulk region, β is the kinetic coefficient of interface motion, T_A is the temperature of solidification of the system's main component (pure substance), T_0 is the initial temperature in the system, m is the tangent of the liquidus line slope on the diagram of phase state of a binary system, and k is the partition coefficient.

The isothermal conditions of dendritic growth imply that for the characteristic heat conductivity scale $l_T=a/V$, any temperature inhomogeneity in the system is smoothed more rapidly than the concentration inhomogeneities (a is the thermal diffusivity in the system). Thus the latent heat is neglected and the system of equations (1)–(4) describes nonequilibrium solidification in isothermal conditions. Defining the diffusion scale as $l_D=D/V$ (D is the diffusion coefficient) and evaluating $D/a\sim10^{-2}$ for nonmetallic substances and $D/a\sim5\times10^{-4}$ for metallic ones, we can get the estimate $l_D/l_T\ll1$. Therefore, the present modeling is restricted by regions whose space scale is essentially larger than the diffusion mass transfer scale but limited by the temperature conductivity scale.

The model we consider is a special case in which the liquid-solid surface tension equals zero under deep undercoolings. As it has been shown in Ref. [3], the kinetics of the particle attachment to the growth surface has a stabilizing action on the growth velocity and the shape of the free dendrite under large undercoolings in the system. In such a case, the only physical parameter that defines the solution of Eqs. (1)–(4) is the dimensionless undercooling $\delta T_0=(T_A-T_0-mC_0)/T_Q$, where C_0 is the initial concentration of the solute component in the binary system, $T_Q=Q/\varkappa$ is the temperature of adiabatic solidification, Q is the latent heat of solidification, and $\varkappa$ is the heat capacity.

We obtained the solution of Eqs. (1)–(4) by the finite-difference technique on the two-dimensional square lattice. A detailed numerical method of solution of the system of equations (1)–(4) was developed in the monograph [1] (see pp. 137–143 in Ref. [1]). It should be noted that at high undercoolings the stabilizing action of the surface energy may be neglected and also imitated by the anisotropic influence of the computational lattice [1]. In such a case, the only computational parameter that influences the structure formation is the space lattice scale [1].

In the calculations we chose the next physical constants applicable to the metal-like binary system: $T_A=1809$ K, $C_0=0.1$ wt. %, $m=80$ K/wt. %, $k=0.1$, $D=6\times10^{-8}$ m^2/s, $Q=10^9$ J/m^3, $\varkappa=5\times10^6$ J/(m^3 K), and $\beta=0.4$ m/(s K).

We chose the scaling length as $h_D=D/V_0$, the time scale as $\tau_D=D/V_0^2$, and the scale velocity as $V_0=\beta T_Q$. The time interval τ of the simulation was chosen as $0.18\tau_D$ and the lattice scale $h=2(D\tau)^{1/2}<h_D$, where h_D is the upper limit of the lattice scale h.

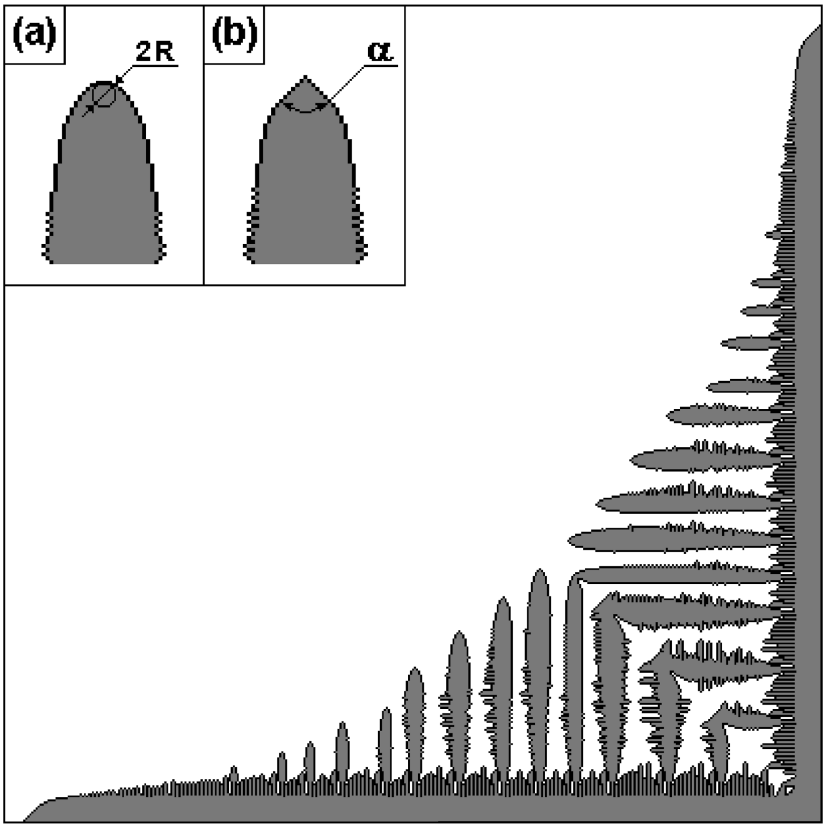

FIG. 2. Coarsening structure at the later stage of the dendrite sidebranch surface formation $\delta T_0=1.39$. The calculation was done on the 451×451 lattice. The initial seed of the solid phase was chosen at the right corner of the lattice. The inset shows (a) the smooth nearly parabolic shape near the dendrite tip, which is characterized by the radius R and (b) the angled dendrite with the angle α.

Taking into account these relations for scaling values and the model constants adopted above, the lattice scale h becomes comparable to the value with the diffusion scale h_D: $h=0.85h_D$. The inequality $h<h_D$ guarantees the appearance of the dendrite structure determined by both the kinetics on the growth surface and the diffusion in the liquid.

By introducing the variable G that defines the phase state (liquid, $1-G$, or solid, G) of the system at each point and its governing equation (2), one can apply numerical methods that avoid the interface moving with the velocity V [see Eq. (3)]. Since the liquid-solid interface width has a distance of several atomic dimensions [12], we calculated the region between the phases as a solidifying liquid-solid layer ($0<G<1$) that has one lattice scale $h=v/\omega$ [1,3] [see Eq. (2)]. Therefore, the value of the lattice scale h was chosen to be not smaller than some interatomic distance. That is the lower limit of the lattice scale h. In such a case, the discrete finite-difference analog of Eq. (1) describes the diffusion in the liquid ($G=0$) and solidifying liquid-solid layer ($0<G<1$), which represents the liquid-solid interface.

In our lattice model the simulation of the growth process has been carried out according to the following rule [1,3,13]: the solid phase can grow only on the solid phase formed before and a nucleation of crystals ahead of the solidification front is excluded. On the boundary of the lattice domain the condition of mass transfer being absence is set. At any point of the solid phase the concentration remains the same during the modeling and is described by Eq. (4). Thus Eqs. (1)–(4) describe the deterministic model of nonequilibrium growth patterns that can evolve with fourfold symmetry on the square computational lattice.

III. RESULTS OF MODELING

Figures 1 and 2 show the modeling results of typical dendritic patterns grown at different undercoolings. Figure 1(a) clearly illustrates the transition from a compact to a branching crystal structure with fourfold symmetry as the crystal grows larger. A similar change within cluster growth morphology is well known when the crossover from a compact cluster to a fractal structure can occur in isotropic systems [14].

The result of the dendrite origin under a higher undercooling is shown in Fig. 1(b). The initial dense branching structure on the main stems becomes unstable and the coarsening process begins. This process is characterized by the appearance of fast-growing secondary branches. Evolution of the coarsening process leads to the origin of the large secondary branches on dendritic sidebranch surfaces (see Fig. 2).

During the modeling, we observed a transition from the smooth nearly parabolic shape near the dendrite tip to a sharp dendrite tip with planar areas away from it. The latter is the so-called angled dendrite that was obtained within the framework of the local model of the boundary layer [15]. As in the analytical treatment [15], we also noticed that there was a critical undercooling at which an angled dendrite with planar areas behind the tip grew instead of a dendrite with a smooth, nearly parabolic shape (see the inset in Fig. 2). The

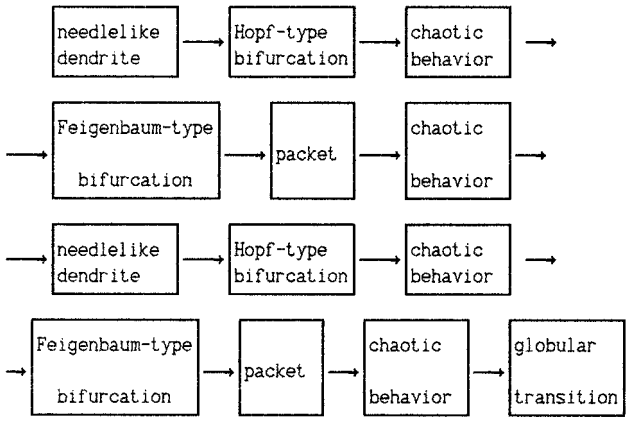

FIG. 3. Scheme of the development of the sidebranch surface of a free dendrite with the increase of the initial undercooling δT_0 in a binary dilute system. The arrows show the direction of the undercooling δT_0 increase. The ''needle-dendrite–packet'' cycles in the ranges $0.69 \leqslant \delta T_0 \leqslant 1.065$ and $1.08 \leqslant \delta T_0 \leqslant 1.14$ are shown. The needle dendrite grows at $\delta T_0 = 0.69, 1.08$; the Hopf bifurcation occurs at $\delta T_0 = 0.89, 1.09$; the Feigenbaum bifurcation occurs at $\delta T_0 = 1.04, 1.12$; the packet origin is at $\delta T_0 = 1.065, 1.14$; chaos occurs at $\delta T_0 = 0.94, 1.075, 1.11, 1.165$; and the globular transition occurs at $\delta T_0 \geqslant 1.20$.

planar areas behind the tip have a certain angle α between them [Fig. 2, inset (b)]. The value of this angle α depends on undercooling and we observed an angle between planar areas up to $\alpha = 90°$ [see the dendritic tips that are at right angles in Figs. 1(b) and 2].

Then, at some new critical undercooling the transition from the branching structure of the surface to a morphologically smooth crystal structure occurs (it is a so-called globular transition; see Refs. [1–3]). An analogous behavior of the dendrite surface area behind the tip has also been considered by means of the local model of the boundary layer [15].

IV. MORPHOLOGICAL SPECTRUM OF A FREE DENDRITE

For a detailed study of the dendrite sidebranch surface we consider the growth from an initially smooth planar front with one perturbation, i.e., with a single solid seed on it. Having the better conditions for the growth, the seed perturbation grows faster than the planar front. The main solidification front retards progressively because of buildup of solute ahead of it. The result is the evolved structure of the dendritic type that forms under the conditions of a small influence from the concentration field ahead of the main solidification front.

We calculated patterns on the 181×181 lattice in the region of undercoolings: $0.5 < \delta T_0 < 1.2$. Figure 3 shows schematically the evolution of the sidebranch surface, i.e., the secondary branches along the main stem of the dendrite versus the initial undercooling in the system.

During the sidebranch surface formation the number of structure bifurcations depends on the initial undercooling. As the undercooling increases, the surface of the needlelike crystal [see Fig. 4(a)] becomes unstable and undergoes a Hopf-type bifurcation. The result is the formation of the dense structure of the secondary branches with the identical space period λ [see Fig. 4(b)]. In our model we obtained that $\lambda = 2h$, i.e., the Hopf-type structure bifurcation leads to the period between the secondary branches, which is equal to the doubled lattice scale.

A further increase in the undercooling leads to a random structure in the sidebranch surface (chaotic behavior in Fig. 3). This chaotic stage is shown by the different, not constant, branching period occurring in the secondary structure of branches along the main stem of the dendrite. Then the dendrite with the doubling period 2λ between the secondary branches occurs [see Fig. 4(c)]. Every second branch slows down by its growth velocity and every other second branch will grow faster. It is clearly a Feigenbaum scenario in the structure formation [3]. It should be noted that in this scenario the period λ between branches is equal to $3h$ and between the fast growing branches the period is $2\lambda = 6h$. The increase in undercooling leads not only to a new bifurcation in the sidebranch surface but also to an increase in the period between branches. The similar behavior $2\lambda = 6h$ of the period doubling along the main stem of the dendrite at different undercoolings was obtained in the model of growth of the heat dendrite in a pure substance [3]. Thus, in our model, the structure transition in the sidebranch surface of the dendrite covers the way from the Hopf-type bifurcation to the Feigenbaum bifurcation through the chaotic stage (see Fig. 3).

As the initial undercooling increases, a structure of the sidebranch surface arises, which we called ''a packet structure.'' In the morphological spectrum the packet structure obtained is in the wake of the structure after the Feigenbaum structure bifurcation (see Fig. 3). The packet structure of the sidebranch surface has the form of the fast-growing branches between which a close-packed structure of slow-growing secondary branches is situated [see Fig. 4(d)].

After the chaotic behavior in the structure of the secondary branches at the undercooling $\delta T_0 = 1.075$, the cycle from the needle crystal up to the packet structure recurs (see Fig. 3). The first cycle, the needlelike-dendrite–packet structure, was obtained in the range of undercoolings $0.69 \leqslant \delta T_0 \leqslant 1.065$. We observed the same second cycle in the range $1.08 \leqslant \delta T_0 \leqslant 1.14$. After the cycle and chaotic behavior in the secondary structure of branches at $\delta T_0 = 1.165$, the globular transition occurs at the undercoolings $\delta T_0 \geqslant 1.20$ (see Fig. 3). We observed the globular transition as a transition to the morphologically smooth growth front.

V. DISCUSSION

Considering the morphological spectrum of the dendrite sidebranch surface, we chose intentionally relatively small calculating domains (181×181 lattice sites; see Fig. 4) that were also limited by the temperature conductivity scale (see Sec. II). In essence, we show the results of the evolved sidebranch surfaces that were formed during the initial stages of solidification. Indeed, if one follows the evolution of the dendritic structure on the larger calculating domains, it is possible to discover the fast-growing secondary branches origin in the dense structure of the secondary branches [compare the dendritic structures in Figs. 4(b), 1(b), and 2]. It is a coarsening process in growth form. As a rule, the distance between these secondary fast-growing branches is not defined by a number that is a multiple of the doubled period,

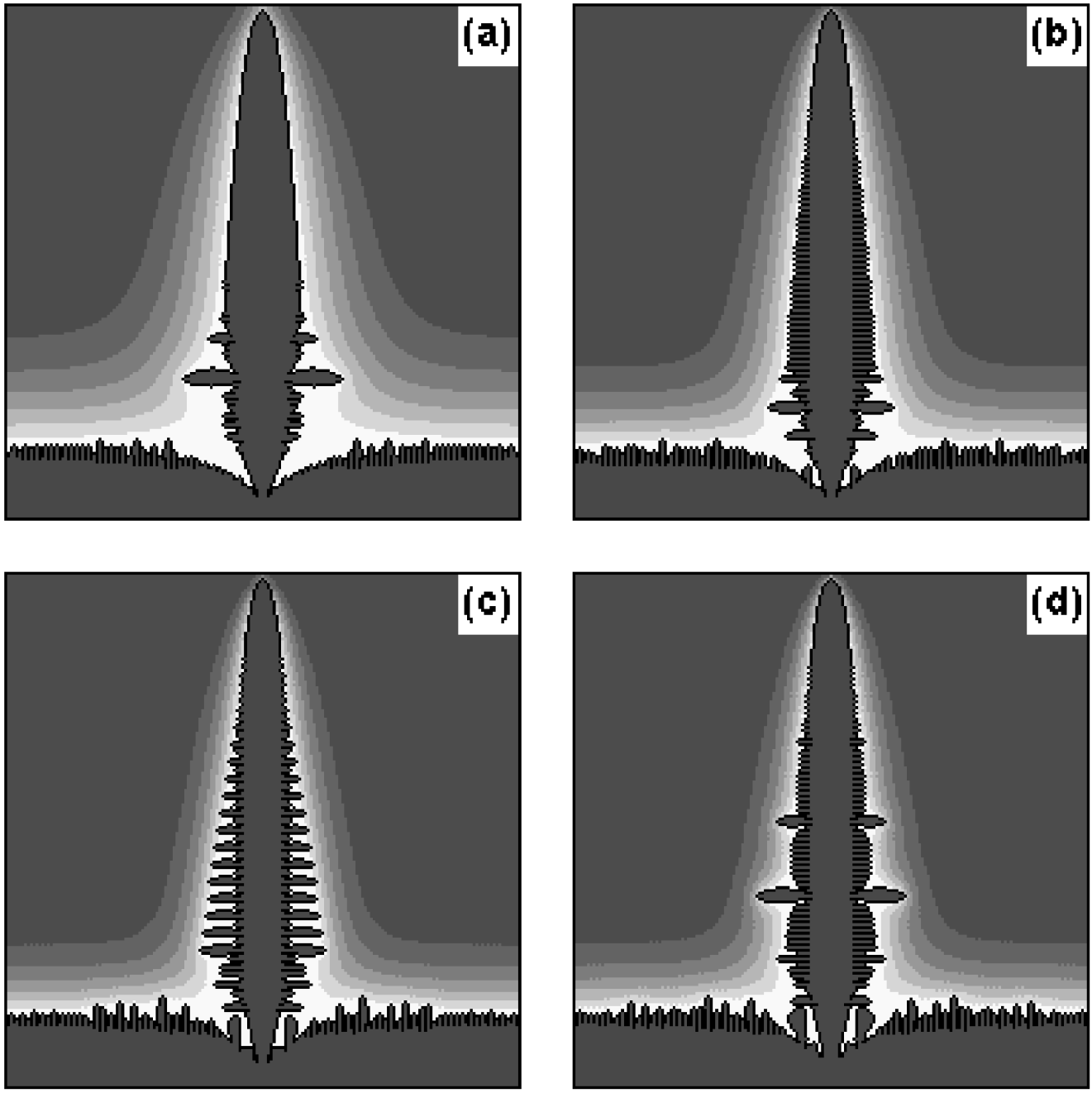

FIG. 4. Illustration of the different types of free-growing dendritic structures in the two-dimensional computer model: (a) a needlelike dendrite at $\delta T_0=0.69$, (b) a dendritic structure after a Hopf-type bifurcation in the sidebranch surface at $\delta T_0=0.89$, (c) a dendritic structure after a Feigenbaum bifurcation in the sidebranch surface at $\delta T_0=1.04$, and (d) a packet structure of the dendrite sidebranch surface at $\delta T_0=1.065$. Close to the dendritic surfaces, the concentration field in the liquid decreasing in the direction from light to dark color is shown.

i.e., more complex structures at the late stages of the crystal growth origin. As it was established in Liu and Goldenfeld modeling [13], in the complex crystal growth process at the late stage, both the nonlinear and the steady-state selection principles are present. As applied to the results of our modeling, this means the following. First, the tip is stable and the crystal surface is unstable (the steady-state selection principle or, in other words, the marginal stability principle [6,7]). Second, the coarsening process is conditioned by the interaction of the diffusion fields between the secondary branches (nonlinear selection principle).

Within the limits of the adopted assumptions and model constants the results of the present modeling clearly demonstrate that besides the evolution of the secondary branch structure realized by regularly repeated doubling of distances between the secondary branches, there is a clear tendency for the formation of structures with random branching period, packet structures with the branching period that is not defined by the Feigenbaum scenario, needlelike crystal, and the structure after the Hopf-type bifurcation (see Figs. 3 and 4). This variety found in the discrete finite-difference analog of the continuum model (1)–(4) exhibits not only the mechanism of sequential period doubling as at the coarsening structure stages in a continuum isolated adiabatic system (see Ref.

[11]), but also other mechanisms of the dendrite surface formation (see Fig. 4). In the present investigation when the binary dilute system solidifies under isothermal conditions, it is possible to suppose that near the hypercooling $\delta T_0 \cong 1$ or behind the hypercooling $\delta T_0 > 1$ the nearly adiabatic system and the adiabatic system are realized, respectively. The conserved quantity in the system is $C_0 = N^{-1}\Sigma[(1-G)C_L + GC_S]$, where Σ is the sum over all lattice sites and N is the total number of lattice sites. The results of our modeling (see Figs. 3 and 4) indicate that the solidifying binary system has a crystal growth scenario in which the period doubling in the dendrite sidebranch surface is not the only possible one. For example, the nonequilibrium coarsening process also leads to the packet structure [Fig. 4(d)]. The answer is the adjustment of the structure according to both the undercooling and the lattice scale.

When the shape of needlelike crystal [Fig. 4(a)] is carried out beyond the threshold of morphological stability [1,2,5–7,13] the origin of the secondary branches occurs [Fig. 4(b)]. The distance between them is λ. In our model we obtained that $\lambda = 2h$ [Fig. 4(b)], i.e., the Hopf-type structure bifurcation leads to a period between the secondary branches equal to the doubled lattice scale. This is explained by the fact that the lattice scale h chosen by us was a little smaller than the diffusion scale h_D that defines the scale of local instability in the growth form. If one accepts $h^* \cong 0.5h_D$, it is possible to see that after the same modeling time the numerical value of the distance between the secondary branches after the Hopf-type bifurcation remains the same, i.e., $\lambda = 4h^* \equiv 2h$.

An interaction of the diffusion fields of neighboring branches leads to nonequilibrium coarsening of the secondary branches [see Fig. 4(c)]. This phenomenon consists in the fact that every second branch slows down in its development and after some time may be ''caught'' by a neighboring branch. As a result, the distance between fast-growing branches increases and becomes equal to the period $2\lambda = 6h$. The chaotic regime, as an adjustment of the structure according to the undercooling and simultaneously to the lattice scale, leads to the next type of bifurcation: the Hopf-type structure bifurcation gives way to the Feigenbaum scenario (see Fig. 3). A further increase in the undercooling and interaction of the diffusion fields between the secondary branches lead to a nontrivial coarsening of the sidebranch surface, i.e., to the packet structure of the secondary branches. The distance between fast-growing branches within the packet structure can be different and, generally speaking, not a multiple of bifurcations of the period doubling. Thus the different types of crystal structures may depend on the lattice scale h and the initial undercooling δT_0 in a binary system (see also pp. 125–127 and Fig. 4.4 in Ref. [1]).

In the behavior of structures of the growing crystals, usually three dynamic regimes are distinguished [16]: the nearly equilibrium behavior (nonequilibrium crystal, the shape of which is defined by the Curie-Wolff rule), the ordering structure origin (fine snowflake forms), and the random structure origin (crystals with random period of branching or fractals). All these three types of structures were obtained in our model. However, they are distributed in such a way that the double structure cycle, the needlelike-dendrite–packet structure, occurs before the globular transition (Fig. 3).

A plausible explanation of the double structure cycle follows. As is well known, when the surface tension is zero or isotropic and surface kinetics is isotropic, dendritic growth does not occur, but rather tip splitting of growing fingers [5,8,16,17]. With both surface tension and anisotropy present, the unique stable needle crystal is selected from the continuous family of analytical solutions found by Ivantsov [18] and a dendrite having the secondary branches grows with the velocity equal to the maximum value of the velocity from the family [9,19]. Notwithstanding the fact that in our statement of the problem we assumed a zero surface tension, an anisotropy of surface kinetics was set by us at the level of the computational lattice as soon as we passed from continuum equations (1)–(4) to their finite-difference analogs. This leads to the dendritic growth of the crystal without tip splitting. Furthermore, the continuous family consisting of the needlelike crystals, dendrites after Hopf and Feigenbaum bifurcations, and the packet structures is the spectrum of virtual crystal structures. From this continuous family the unique structure is selected at fixed undercooling. As the needlelike shape of the dendrite is selected from the continuous family of the solutions [9,19,20], the present numerical solution also gives the discrete family of the above structures. Thus, for every virtual structure we obtained the discrete family of stable growth form in the continuous family of the numerical solutions (see Fig. 3).

In contrast to various investigations in which the tip radius was calculated in detail (see, for example, Refs. [2,5]) by means of the well-known Ivantsov solution for a parabolic dendrite [18], in our investigation the shape near the tip was not parabolic. In our model the shape near the tip became nearly parabolic in the region $0.05 < \delta T_0 < 0.1$, while in the process of growth of the dendrite the current undercooling $\delta T = (T_A - T_0 - mC_L)/T_Q$ on its surface gradually decreased practically to zero. (In the region of the initial undercoolings $\delta T_0 < 0.005$ the growth of the dendritic branches was accompanied by the splitting of its tip). In this connection, for the statement of the behavior of the tip growth we calculated the total area of a certain nonbranching region behind the tip.

During the growth process we calculated the area of the nonbranching region all the way from the tip up to $7h$ from it. We calculated the solid fraction G in all lattice sites that were occupied by the solid ($G = 1$) and the liquid-solid ($0 < G < 1$) phases. Shown in Fig. 5 is a dependence of the area Σ_T near the dendrite tip versus the modeling time t_M. Here Σ_T is the area equal to the total value of the solid phase in the solid and liquid-solid sites of the nonbranching region near the tip and t_M is the time equal to the quantity of the numerical steps τ of simulation.

We distinguished three stages in the evolution of the crystal: the nonbranching compact crystal, the developed dendritic crystal, and the final stage of growth on the calculating domain. These time intervals from A to C are shown in Fig. 5. It can be seen that the area near the dendrite tip oscillates about some steady-state value. This area oscillates with time intervals determined by the beginning of the next branching on the surface of the dendrite. An analogous oscillation dependence was found in the continuum diffusion-limited aggregation model with anisotropic surface tension [21] and in the model of three-dimensional heat flow dendrites [22].

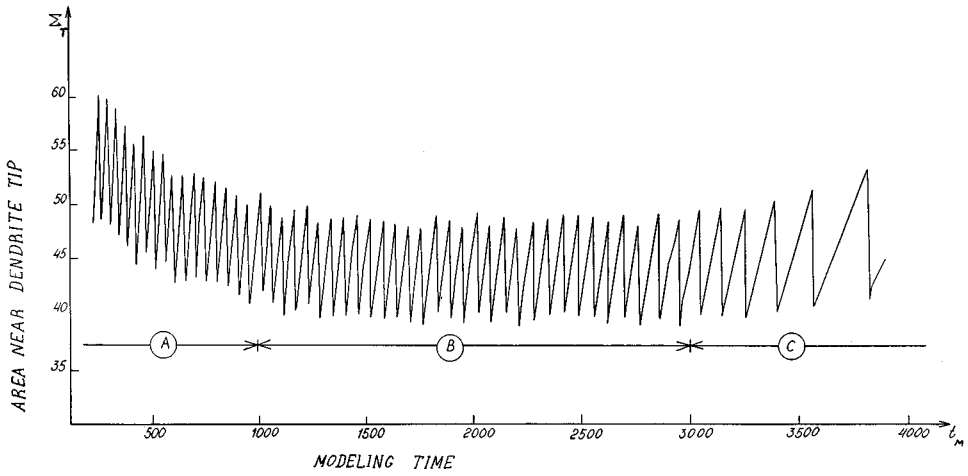

FIG. 5. Dependence of the area Σ_T of the nonbranching region behind the dendrite tip on the time t_M of numerical simulation. The initial undercooling $\delta T_0=0.24$. Here A is the time period where the compact crystal grows, B is the time period of the developed dendrite growth, and C is the time period where the final stages of the dendrite growth occur within a calculating domain.

To try to smooth these oscillations, we also calculated Eqs. (1)–(4) on a half time step 0.5τ. However, oscillations in Σ_T remained the same by amplitude and their frequency corresponded to the origin of the secondary branches on the main stem of the dendrite as before. If these oscillations are not an artifact of the numerical method and solution of the problem, then we may interpret this result from the physical viewpoint as follows.

Defining the tip velocity numerically, we obtained that the diffusion inside the liquid [see Eq. (1)] and surface kinetics [see Eqs. (2) and (3)] do not have a sharp correlation at one time step τ. In principle, this makes the tip velocity and the crystal shape oscillate near the dendrite tip. Presented in Fig. 6 is a change in the current undercooling $\delta T=(T_A-T_0-mC_L)/T_Q$ at the tip and ahead of it during the stage of dendritic growth (time interval B in Fig. 5). It can be seen that in our time-dependent model the undercooling δT and also the tip velocity V [see Eq. (3)] oscillate weakly. In particular, this means that the accumulation of the substance, its removal, and its surface kinetics do not act simultaneously at the time step τ. Notwithstanding that the domains with the set, approximately similar, ranges of concentration as long as several h do not oscillate on the whole (see the smooth regions in liquid with approximately unified concentration in Fig. 4) the tip concentration, the tip undercooling and the tip velocity change in time (see Fig. 6). The frequency of these changes sharply correlates with the origin of new secondary branches far from the dendrite tip. Arising small secondary branches can disappear quite quickly, ensuring the smooth shape of the needlelike dendrite [see Fig. 4(a)], or they can gradually grow, providing the evolved sidebranch surface [see Figs. 4(b)–4(d)].

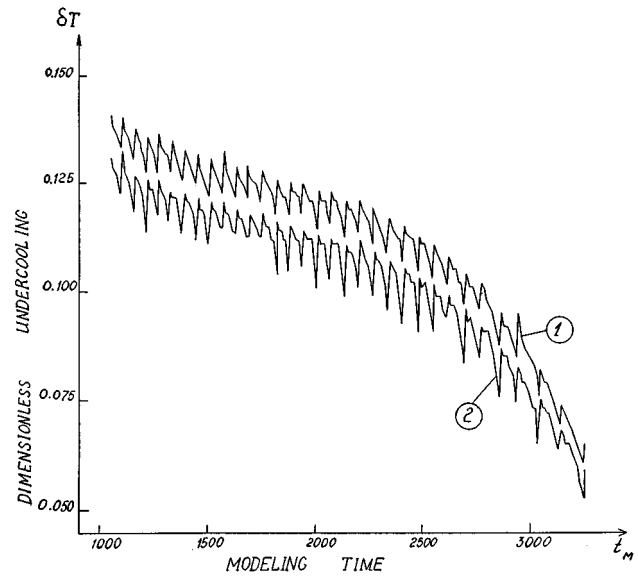

FIG. 6. Current undercooling δT versus the numerical simulation time t_M corresponding to 1, the liquid phase ($G=0$) immediately ahead of the dendrite tip; and 2, the dendrite tip where the liquid-solid phase ($0<G<1$) is present. The initial undercooling $\delta T_0=0.24$.

In Figs. 5 and 6 we demonstrate the oscillations at $\delta T_0=0.24$. Similar oscillations exist under any undercoolings in the system if the kinetic coefficient $\beta=0.4$ m/(s K) adopted above is used. At the same model constants we obtained that the oscillations practically disappear at $\beta<0.005$. This fact is circumstantial evidence for our statement about a not full correlation of the tip surface kinetics and diffusion in the liquid ahead of the tip. Indeed, as soon as the growth kinetics becomes unsufficiently intensive, the diffusion has time to remove the accumulated substance from the surface into the liquid. In this case large, practically nonbranching structures of needlelike crystals grow. These nonbranching structures have been observed in our model under low undercoolings too.

At the undercooling $\delta T_0=0.24$ the value of the frequency of calculated oscillations in the shape near the tip of the dendrite is equal to 10^9 s^{-1}. Therefore, under experimental study these possible oscillations may be observed and fixed only by means of special methods of investigation.

VI. SUMMARY AND CONCLUSIONS

We have presented the results of the numerical study of the isothermal free dendrite growth in undercooled binary dilute liquid. We have used for simulation a time-dependent deterministic model of dendritic solidification in which the diffusion in liquid and the kinetics of liquid-solid interface motion have been taken into account. The numerical solution of the model was obtained by means of the finite-difference technique on the square computational lattice, which made

the growth of dendritic patterns with the fourfold symmetry possible.

We examined different types of sidebranch surfaces of the free-growing dendrite as a result of structure bifurcations. We obtained the morphological spectrum of the dendrite sidebranch surface versus the initial undercooling δT_0 in the region $0.5 \leqslant \delta T_0 \leqslant 1.2$. The increase in undercooling δT_0 leads to the following morphological spectrum: (i) a needlelike crystal, (ii) a dense structure of the secondary branches with the identical space period (structured after a Hopf-type bifurcation), (iii) a random structure (secondary structure of branches with the different, not constant, branching period), (iv) a doubled period between the secondary branches (structured after the Feigenbaum bifurcation), and (v) a packet structure (fast growing branches with the dense structure of slow-growing branches between them). After the random structure of the secondary branches the cycle from the needlelike crystal up to the packet structure recurs before the globular transition. The first, needle dendrite–packet cycle, was obtained in the range of undercoolings $0.69 \leqslant \delta T_0 \leqslant 1.065$ than the second one. We observed the latter in the range $1.08 \leqslant \delta T_0 \leqslant 1.14$.

As the unique needlelike shape of the dendrite is selected from the continuous family of the analytical solutions in the framework of known models of crystal growth (see Refs. [9, 19, 20]), the results of the numerical investigations presented also give the continuous family (i)–(v) of structures from which the unique structure is selected. Several unique selected structures are the discrete spectrum within the continuous family of the above structures (see Fig. 3).

In addition, we have found oscillations in the shape of the nonbranching smooth region behind the tip during the moments of the secondary branches' origin. These oscillations have a continuous character at all stages of crystal growth even if the secondary branches disappear on the stage of compact crystal growth or when the needlelike crystal grows in a system. From the physical viewpoint their existence may be interpreted as a result of the difference between the rate of the diffusion mass transfer near the moving interface and the rate of the surface kinetics.

We have centered on the fact that application of the finite-difference technique to obtaining the continuum model solutions leads to the formation of structures due to both the undercooling and the scale of the computational lattice. First, ignoring surface tension under high undercoolings, we have shown that the tip of the dendrite grows without its splitting because the growth kinetics and also the anisotropic influence of the computational lattice have stabilizing actions on the tip growth velocity. This result is in good agreement with previous works [2,5,10,17,19,20], where it has been shown that anisotropy is required in the interfacial dynamics to produce dendritic growth. Second, we have reason to suppose that a structure such as the random structure in the secondary branches may be defined by the adjustment of the sidebranch surface according to the lattice scale. Here we approached the problem of the adequate reproduction of structures in continuous systems during phase transitions. As it is known, the introduction of stochastic parameters, i.e., fluctuations into a deterministic model, allows one to model quite adequately complex patterns such as those that are observed in nature and experiments. Ignoring fluctuations, in a completely deterministic model, it is apparently necessary to set a correlation between the lattice scale h and the scales responsible for the development of structures (in the present model the diffusion scale h_D is such a scale) *a priori*. In this case a satisfactory comparison of modeling data with the characteristics of natural structures can be obtained. Therefore, the present numerical results may also be examined as a stimulus for a detailed investigation of the lattice scale effect on the pattern formation in the discrete analogs of continuum models. The results presented are certain to be useful for the interpretation of the natural experiments in which the above bifurcations in secondary branching will be observed.

ACKNOWLEDGMENTS

This research was made possible in part by Grant No. J5F100 from the International Science Foundation and Russian Government. P.K.G. thanks the International Atomic Energy Agency and UNESCO for the kind hospitality at the International Center for Theoretical Physics, Trieste, Italy, where part of this work was carried out.

[1] P. K. Galenko and V. A. Zhuravlev, *Physics of Dendrites* (World Scientific, Singapore, 1994).

[2] S.-C. Huang and M. E. Glicksman, Acta Metall. **29**, 701 (1981); **29**, 717 (1981); E. Ben-Jacob, Contemp. Phys. **34**, 247 (1993).

[3] A. R. Umantsev, V. V. Vinogradov, and V. T. Borisov, Kristallografia **30**, 455 (1985) [Sov. Phys. Crystallogr. **30**, 262 (1985)]; **31**, 1002 (1986) [**31**, 596 (1986)].

[4] F. Family, D. E. Platt, and T. Vicsek, J. Phys. A **20**, L1177 (1987).

[5] Y. Saito, G. Goldbeck-Wood, and H. Müller-Krumbhaar, Phys. Rev. A **38**, 2148 (1988).

[6] J. S. Langer and H. Müller-Krumbhaar, Acta Metall. **26**, 1681 (1978).

[7] J. S. Langer, Rev. Mod. Phys. **52**, 1 (1980); A. Karma and J. S. Langer, Phys. Rev. A **30**, 3147 (1984).

[8] T. Vicsek, *Fractal Growth Phenomena*, 2nd ed. (World Scientific, Singapore, 1992).

[9] A. Karma and B. G. Kotliar, Phys. Rev. A **31**, 3268 (1985).

[10] D. A. Kessler and H. Levine, Phys. Rev. A **39**, 3041 (1989); C. Misbah, H. Müller-Krumbhaar, and Y. Saito, J. Cryst. Growth **99**, 156 (1990).

[11] A. Umantsev and G. B. Olson, Phys. Rev. E **48**, 4229 (1993).

[12] J. Q. Broughton, A. Bonissent, and F. F. Abraham, J. Chem. Phys. **74**, 4029 (1981); S. J. Cook and P. Clancy, *ibid*. **99**, 2175 (1993).

[13] F. Liu and N. Goldenfeld, Phys. Rev. A **42**, 895 (1990).

[14] P. Meakin, F. Family, and T. Vicsek, J. Colloid Interface Sci. **117**, 394 (1987).

[15] E. A. Brener and D. E. Temkin, Europhys. Lett. **10**, 171 (1987).

[16] L. M. Sander, in *Fractals in Physics*, Proceedings of the Sixth

International Symposium of the ICTP, Trieste, 1985, edited by L. Pietronero and E. Tosatti (North-Holland, Amsterdam, 1986).

[17] E. Ben-Jacob, N. Goldenfeld, J. S. Langer, and G. Schön, Phys. Rev. Lett. **51**, 1930 (1983).

[18] G. P. Ivantsov, Dokl. Akad. Nauk SSSR **58**, 576 (1947); **83**, 573 (1952).

[19] E. Ben-Jacob, N. Goldenfeld, B. G. Kotliar, and J. S. Langer, Phys. Rev. Lett. **53**, 2110 (1984); D. A. Kessler, J. Koplik, and H. Levine, Phys. Rev. A **31**, 1712 (1985).

[20] J. S. Langer, in *Chance and Matter*, 1986 Les Houches Lectures, Session XLVI (Elsevier, New York, 1987); E. A. Brener, S. V. Iordanskii, and V. I. Melnikov, Zh. Eksp. Teor. Fiz. **94**, 320 (1988) [Sov. Phys. JETP **67**, 2574 (1988)]; E. A. Brener and V. I. Melnikov, Adv. Phys. **40**, 53 (1991).

[21] L. M. Sander, P. Ramanlal, and E. Ben-Jacob, Phys. Rev. A **32**, 3160 (1985).

[22] J. D. Hunt, Acta Metall. Mater. **39**, 2117 (1991).